AIAA JOURNAL
Vol. 30, No. 11, November 1992

Optical Microphone for the Detection of Hidden Helicopters

Cecil F. Hess*
MetroLaser, Irvine, California 92714

This paper discusses the characteristics of a laser Doppler microphone used to measure acoustic disturbances in the vicinity of a helicopter and other acoustic radiators. Analytical and experimental work demonstrate that an acoustic radiator impresses upon the atmosphere a fundamental frequency and harmonics that frequency shift the Doppler frequency resulting from the convective air motion. The net effect is the creation of a signature that depends on the acoustic pressure. Since the acoustic pressure is higher near the source, a systematic method could then be implemented to locate the helicopters, namely, the location of maximum acoustic pressure. The reported experimental measurements were conducted in the laboratory using a small speaker as the acoustic radiator and a reference beam laser Doppler system to measure the frequency associated with particle vibration and convection. The illumination was provided by a 40-mW diode laser that illuminated incense particles entrained in a controlled atmosphere. The signal was Fourier transformed and the results were compared to an analytical model. Acoustic frequencies between 100 Hz and 400 Hz were measured with a typical accuracy of 5%.

Introduction

HELICOPTERS radiate acoustic signatures that are impressed on the surrounding air as well as on objects in the near vicinity (e.g., trees, buildings, and the ground). This paper discusses the requirements and characteristics of an optical microphone that would scan the environment in the vicinity of the helicopter and would produce a signal associated with specific acoustic disturbances. Unlike conventional microphones, optical microphones have superior directionality resolution and, if properly isolated, will not be confused or overwhelmed by the noise in the immediate vicinity.

Acoustic measurements using the Doppler shift of laser light have been described by Taylor,[1] Hanish,[2] and Vignola et al.[3] The present work is aimed at demonstrating that acoustic disturbances can be measured remotely with an optical microphone. Measurements were conducted with a continuous-wave laser Doppler breadboard using a reference beam configuration. The acoustic disturbances were generated in the laboratory with a speaker driven by a function generator.

Velocity measurements were made of submicron-size incense particles entrained in air and of leaves placed in the vicinity of a speaker. The velocity was comprised of the local wind speed and acoustic terms. The Doppler frequency associated with the measured velocity was separated by a digital spectrum analyzer and can be expressed as

$$f_D = |f_c \pm nf_a| \tag{1}$$

where f_c is the frequency due to the convective air motion, f_a is the acoustic frequency of the disturbance, and n is the nth harmonic.

This equation was verified both numerically and experimentally and constitutes the basis of the optical microphone. It indicates that the fundamental frequency of the acoustic radiator is not readily measured except in the rare case in which the wind velocity is zero. In general, the acoustic generator (i.e., the helicopter) may be located by systematically optimizing the number of harmonics measured by the Doppler system. As indicated in the following, the number of harmonics is a function of the particle displacement that is proportional to the acoustic pressure. The optical microphone would ultimately employ a pulsed laser Doppler lidar system because of the need for high power and spatial discrimination.

Numerical Analysis

The laser Doppler system uses a reference beam configuration where the signal and reference beams heterodyne on the detector. There are no fringes formed in the probe volume, but the system may be modeled by defining a virtual fringe spacing δ given by

$$\delta = \lambda/2 \sin(\gamma/2) \tag{2}$$

where λ is the laser wavelength, and γ is the angle of intersection between the object and reference beams.

A particle traveling through this fringe pattern will scatter light with an amplitude given by

$$I = I_0(1 + \cos 2\pi x/\delta) \tag{3}$$

where I_0 is the peak fringe intensity, and x is the distance measured from the start of any of the cycles. Note that the intensity distribution of the laser beam cross section is neglected for the purpose of this analysis.

A particle that is moving with the medium at a velocity V and by the oscillation produced by a periodic acoustic wave with rotational frequency ω_a will move a distance x, given by

$$x = Vt + X_m \cos(2\pi\omega_a t) \tag{4}$$

where X_m is the maximum displacement due to the acoustic motion.

Substituting Eq. (4) into Eq. (3), one obtains the final expression:

$$I = I_0\{1 + \cos[2\pi/\delta[Vt + X_m \cos(2\pi\omega_a t)]]\} \tag{5}$$

This expression was Fourier transformed for a series of parameters, and the resulting frequencies can be summarized by Eq. (1).

Figure 1 shows the spectrum corresponding to a numerically generated signal with convective frequency of 167 Hz and acoustic frequency of 400 Hz. Figure 2 shows similar results but for f_c = 1000 Hz and f_a = 400 Hz. The various peaks on the spectra are labeled in terms of f_c and f_a, and it can be confirmed that they are consistent with Eq. (1).

Presented as Paper 92-0377 at the AIAA 30th Aerospace Sciences Meeting, Reno, NV, Jan. 6–9, 1992; received Feb. 6, 1992; revision received May 4, 1992; accepted for publication May 7, 1992.

*Director of Engineering. Member AIAA.

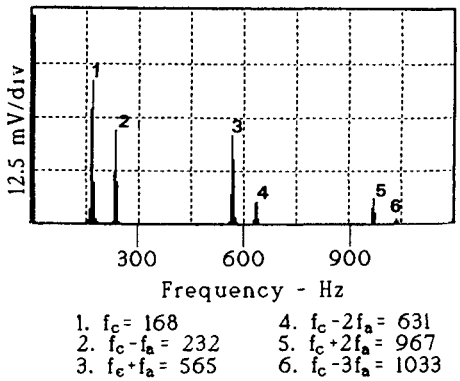

Fig. 1 Spectrum of numerically generated signal with f_c = 167 Hz.

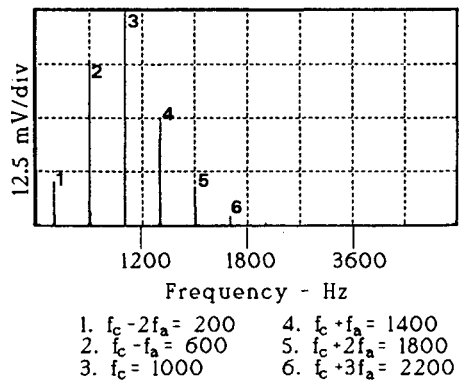

Fig. 2 Spectrum of numerically generated signal with f_c = 1000 Hz and f_a = 400 Hz.

The convective frequency f_c is given by

$$f_c = V/\delta \tag{6}$$

For a traveling longitudinal wave the maximum displacement X_m is given by

$$X_m = P/(k\rho v^2) \tag{7}$$

where P is the acoustic pressure, $k = 2\pi/\lambda$ is the wave number, ρ is the density of air, and v is the velocity of sound.

The wave number can be rewritten as

$$k = 2\pi\nu/v$$

where ν is the frequency of vibration characteristic of the acoustic radiator.

Note that in Eqs. (4–6) the wind velocity V, measured by the optical microphone, is the component perpendicular to the virtual fringes. The displacement X_m is also measured perpendicular to δ. In a monostatic backscattering system the virtual fringes are perpendicular to the laser beam; thus, the component of the wind velocity measured by the optical microphone is along the beam trajectory (sometimes this is referred to as the radial velocity component).

To assess the applicability of this technique in detecting helicopters, the following parameters were assumed in estimating the displacement of the surrounding air: ν = 100 Hz, v = 340 m/s, ρ = 1. 22 kg/m^3, and P = 28 N/m^2. The value of P was chosen assuming that the acoustic disturbance right next to the helicopter is equal to the maximum pressure disturbance tolerable by our ears (i.e., 28 N/m^2).

Substituting these values into X_m, one obtains a maximum displacement of 104 μ at the helicopter source. This longitudinal displacement correlates directly with the pressure disturbance that decays as R^{-1}, where R is the distance from the helicopter to the particles. The laboratory tests discussed in the following show that the laser Doppler microphone can detect disturbances much smaller than 1 μ. This simplified analysis suggests that a laser scan hundreds of meters away from the helicopter would detect its presence.

Experimental Work

Two breadboard configurations were used to characterize the flowfield. The first consisted of a reference beam forward-scattering configuration, and the second consisted of a reference beam backscattering configuration. The backscattering configuration would be the most likely candidate for field work; however, it was more difficult to implement in the laboratory for the following reasons:

1) The low laser power limited the measurement of small incense particles suspended in air.

2) The speaker that produced the acoustic disturbances could not be placed normal to the fringes or close to the probe volume since the reflection from the speaker would overwhelm the signal. Because of these limitations, the speaker had to be driven at a fairly high volume, thus shaking the optical instrument. Under these conditions it was difficult to separate instrument vibration from particle vibration.

3) The Doppler frequency due to air motion (referred in this paper as the convective frequency) was typically very high since the fringe spacing was small. This last difficulty can be overcome by introducing frequency shift to the reference beam.

Signals resulting from collecting either backscattered or forward-scattered light were similar in nature and provided the same qualitative results. However, there are quantitative differences due to the following reasons:

1) The Mie scattering coefficients are much larger on forward scattering, resulting in a larger signal-to-noise ratio. For instance, incense smoke produced an excellent signal in forward scattering, but in backscattering the signal was weak. This could be compensated for by using a more powerful laser, such as a 2-W argon ion laser (see the analysis of the signal-to-noise ratio given in the following).

2) The fringe spacing on forward scattering is about 45 times larger than that in backscattering [see Eq. (2)]. Thus, the frequency corresponding to a given convective velocity would be 45 times smaller. The advantage of a small convective Doppler frequency is that it makes it easier to separate the acoustic frequency from the total. Alternatively, a frequency shift could be introduced on the reference beam to offset a large convective Doppler frequency.

The submicron incense particles were measured both in forward scattering and backscattering but were primarily measured with a forward-scattering reference beam configuration. This configuration allowed the speaker to be placed very close to the probe volume and allowed the suspended particles to be contained in a Plexiglas cell where the convective term of the velocity could be controlled. The speaker was placed inside the cell with the woofer about 3 cm from the probe volume. Most of the backscattering measurements were made on large objects such as leaves.

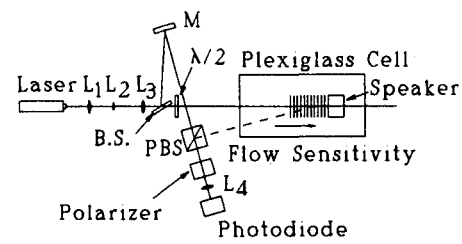

Fig. 3 Schematic of off axis backscattering laser velocimeter.

Laser Velocimeter Breadboard

Backscattering

A breadboard of the laser velocimeter was designed and constructed in the laboratory (Fig. 3). The design was based on a backscattering monostatic system in which a diode laser provided the required illumination and polarizing components optimized the throughput. The diode laser (Melles Griot model 06DLL707) produced up to 50 mW of 815-nm radiation. Its temperature and power were regulated to ensure single mode lasing. The polarization of the beam was horizontal, which corresponded to the p component of the cube beam splitter. A half-wave plate rotated the polarization of the object beam to the vertical or s direction. A thick glass window split the beam into a reference and object beams. Two lenses, especially coated for diode lasers, focused the object beam on the target. The reference beam was folded to match the pathlength of the return object beam. A polarization beamsplitter (PBS) mixed the reference beam and return signal and sent them to the photodiode. The PBS was slightly off axis to avoid the back reflections from the object beam. A Glan Thompson polarizer mixed the object beam with the reference beam, interfering the two at 45 deg over the face of a photodiode. A lens, L_3, was used to focus the light onto the photodiode.

Forward Scattering

A reference beam forward-scattering breadboard was also constructed (Fig. 4). As described earlier, two lenses (L_1 and L_2) focused the object beam on the target. A beamsplitter separated the object and reference beams. The reference beam passed through a neutral density filter, which attenuated it to about 5%. This reference beam was directed into the photodiode via a focusing lens (L_3). The object beam was directed to the probe volume. Light scattered from the probe volume was collected by L_3 and also focused on the photodiode. Thus, the reference beam and the scattered light heterodyne on the face of the detector.

Forward-Scattering Experiments

The first set of experiments established the combinations of acoustic frequency and speaker volume that would not vibrate the breadboard. A piece of glass was placed in the probe volume, and the light scattered from its surface was mixed with the reference beam on the photodetector. Different combinations of speaker frequency (from 100 Hz to 600 Hz) and volume were tried while the signal from the photodetector was measured, thus defining the operational envelope.

In the second set of experiments the glass was removed from the probe volume and incense sticks were burned inside the cell. After a reasonably steady-state condition was obtained, the airflow was measured with no sound. This flow ranged from almost stationary (~ 1 mm/s) to slowly moving (~ 20 mm/s). The former was obtained by letting the incense stand for a while, and the latter was obtained from the natural convection of the incense as it burned. After the Doppler frequency spectrum was recorded, the speaker was turned on, and various frequencies and volumes were tried within the established operating envelope.

It should be pointed out that, although no attempt was made to measure the incense concentration, excellent signals could be obtained even after most of the incense had escaped from the box and its inside appeared transparent to the eye.

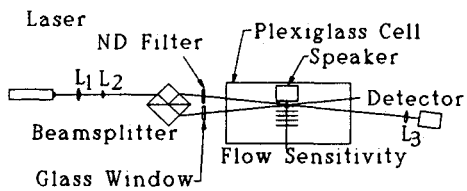

Fig. 4 Forward-scattering reference beam probe.

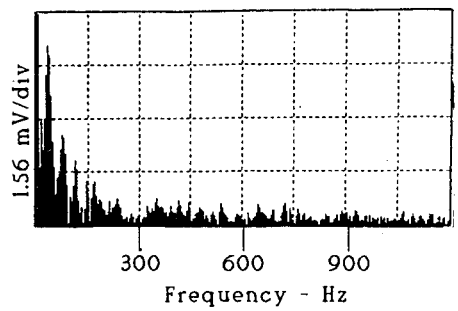

Fig. 5 Forward-scattering signal of near stagnant incense with no acoustic disturbance.

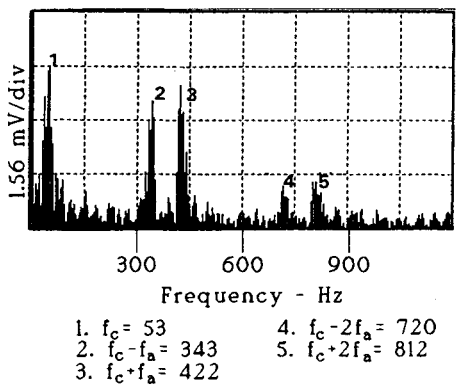

Fig. 6 Forward-scattering signal of near stagnant incense with acoustic signal of 400 Hz, −10 dB.

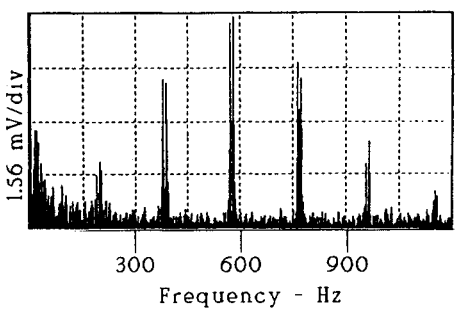

Fig. 7 Forward-scattering signal of near stagnant incense with acoustic signal of 400 Hz, 0 dB.

The spectra corresponding to some of the conditions are given in the following.

Figure 5 corresponds to an almost stagnant incense with no acoustic disturbance. Thus, the frequency shown is the convective Doppler frequency, which in this case peaks around 35 Hz, indicating a very low velocity of 0.65 mm/s.

In Fig. 6 the incense was almost stagnant and the speaker was driven at ~ 400 Hz and ~ −10 dB. The values of the peak frequencies are indicated on the figure. Notice the presence of harmonic frequencies and the double peaks. They can be explained by recalling that the spectrum should be characterized by frequencies at $|f_c \pm nf_a|$. Thus, the first peak of ~ 53 Hz would be f_c, the second peak of 343 Hz would be $|f_c - f_a|$, the third peak of 422 Hz would be $|f_c + f_a|$, the fourth peak of 720 Hz would be $|f_c - 2f_a|$, and the fifth peak of 812 Hz would be $|f_c + 2f_a|$.

The distance between any pair of peaks would be $2f_c$. Solving from these data, we obtain f_c = 40–45 Hz and f_a = 384 Hz. This f_c value is about 10 Hz lower than the first peak, and f_a is 16 Hz lower than the driven acoustic frequency that is within experimental error.

In Fig. 7 the incense was almost stagnant and the speaker was driven at ~ 400 Hz and 0 dB. The fundamental plus five

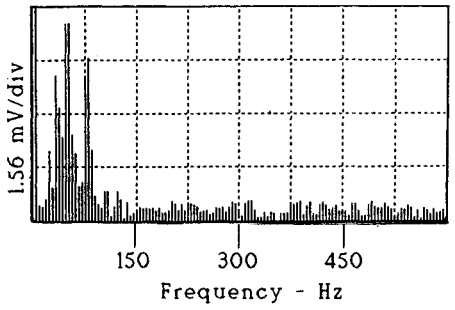

Fig. 8 Forward-scattering signal of slow moving incense with no acoustic disturbance.

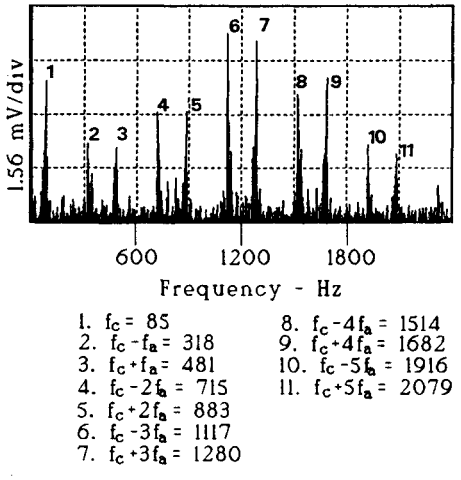

Fig. 9 Forward-scattering signal of slow moving incense with acoustic signal of 400 Hz, 0 dB.

harmonics are displayed on the spectrum. Notice that the double peaks are separated by 20 Hz, which corresponds to $2 \times f_c$. The acoustic frequency may be inferred from the harmonics as $f_a = 387$ Hz.

Figure 8 corresponds to slowly moving incense with the speaker off. The spectrum of the convective Doppler frequency is shown on the figure.

Figure 9 shows the incense moving at approximately the same velocity as that in Fig. 8, but here the speaker is on at 400 Hz, 0 dB. This is a textbook example of how the various harmonics are frequency shifted by $\pm f_c$. The difference between the double peaks is $2 \times f_c$, yielding $f_c = 84$ Hz, which corresponds to the first peak on the spectrum.

Figure 10 corresponds to incense moving at about 20 mm/s and the speaker off. A convective frequency of ~ 1126 Hz can be identified on the spectrum. Notice that with this velocity the particles will remain in the beam for ~ 25 ms (assuming a 500-μ probe volume diameter). For an acoustic disturbance of 400 Hz the particle will cross 10 cycles before leaving the probe volume.

Figure 11 corresponds to incense moving at about the same velocity as that in Fig. 10 and with the speaker on at 400 Hz, -10 dB. This case shows the expected frequencies when the convective term is larger than the acoustic disturbance. The fundamental expression $|f_c \pm nf_a|$ is also valid here, but there can be no closely spaced double peaks as in some of the previous spectra. Instead, the various acoustic harmonics are added and subtracted to the convective frequency. The difference between any two consecutive peaks is simply f_a.

Backscattering Experiments

The receiver of the backscattering breadboard was placed at 170 deg to avoid measuring the reflection from the Plexiglas surface and the speaker. In the experiments reported here the reflecting object was a leaf that could be stationary or could be blowing with the wind.

The following spectra were obtained with the backscattering breadboard:

Figure 12 shows the spectrum of an acoustically excited, virtually stationary leaf. The speaker in this case was driven at ~ 450 Hz. The double peak identified by the cursors corresponds to $|f_c + f_a|$, and to $|f_c - f_a|$. Thus, the difference between the two peaks is $df = 65$ Hz, which should be twice the f_c. Notice the 33-Hz peak shown on the figure, thus confirming our assumption. This would implicate that the acoustic frequency was actually 430 Hz.

Figure 13 corresponds to a leaf that was moving due to a gentle breeze while the speaker was driven at ~ 450 Hz. As before, the fundamental expression that explains the phenomenology is $|f_c \pm nf_a|$. In this case f_c is larger than f_a and three peaks are clearly identified on the spectrum. As indicated on the figure, these peaks correspond to $n = 0$, $n = 1$, and $n = -1$. The difference between two of these consecutive peaks should be the acoustic frequency, which was measured as 449 Hz.

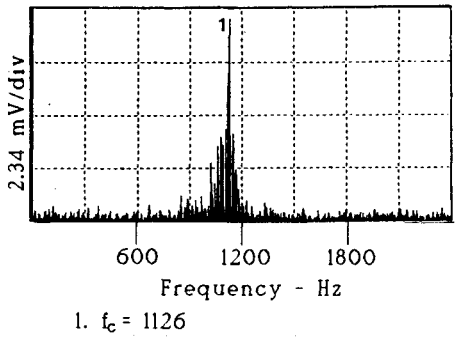

Fig. 10 Forward-scattering signal of fast moving incense with no acoustic disturbance.

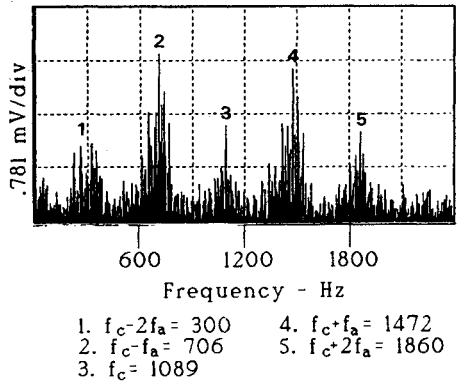

Fig. 11 Forward-scattering signal of fast moving incense with acoustic signal of 400 Hz, -10 dB.

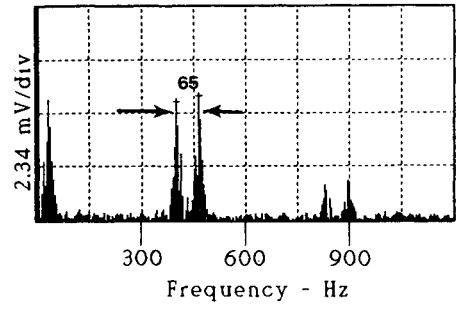

Fig. 12 Backscattering signal of near still leaf excited by acoustic signal of 450 Hz.

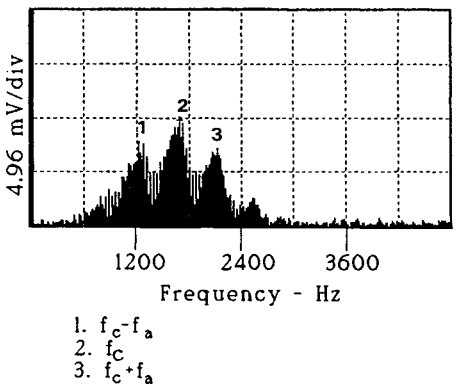

Fig. 13 Backscattering signal of moving leaf excited by acoustic signal of 450 Hz.

In summary, the backscattering signal is qualitatively identical to the forward-scattering signal and the response function can be expressed by $|f_c \pm nf_a|$.

Experimental Errors

A major potential experimental error results from vibrating the optical system with the acoustic radiator. This would cause the optical system to vibrate at the same fundamental frequency that it is trying to measure. Under this condition the signal output would be analogous to the signal corresponding to vibrating particles. Great care must be exercised in acoustically isolating the optical system and in keeping a reasonable distance between the optical system and the acoustic source.

Another major challenge is separating the acoustic frequency from the convective frequency when the latter is much larger than the former. New algorithms are being developed by the author that would allow the convective frequency to be subtracted from the total measured Doppler frequency.

Other experimental errors are the result of signal broadening sources such as unresolved turbulence, velocity gradients within the probe volume, time of flight broadening due to the finite size of the probe volume, and atmospheric scintillation.

Analysis of Signal-to-Noise Ratio

The signal-to-noise ratio was computed for a 2-W argon ion laser operating at 0.5145 μ and a single monostatic system with a 60-mm aperture measuring at a range of 100 m.

To measure over a single speckle, the receiving aperture and the transmitting aperture should be of the same size. For a Gaussian beam,

$$d_w = 4\lambda T/\pi D_L \tag{8}$$

where d_w is the diameter at the waist, T is the throw (100 m), and D_L is the aperture diameter of either the transmitter or the receiver. For the assumed values the diameter at the waist is computed as 1.092 mm.

The peak power in the middle of the laser waist is

$$I_0 = 8P/\pi d_w^2 = 8 \times 2/\pi(1092)^2 = 4.27 \times 10^{-6} \quad \text{W}/\mu^2$$

Assuming a transmitting efficiency of 60%,

$$I_0 = 2.5 \times 10^{-6} \quad \text{W}/\mu^2$$

The collected scattered light depends on the particle size and the number of particles in the probe volume. For a particle diameter of 0.65 μ and an index of refraction of 1.5, the scattering cross-sectional area was computed with Mie scattering as $I/I_0 = 7 \times 10^{-9}\ \mu^2$. Using the value of I_0 computed earlier and assuming a collection efficiency of 50%, the light collected from a single particle is $I = 9 \times 10^{-15}$ W.

The number of particles needed in the probe volume is predicated on the number of photoelectrons needed to arrive on the photocathode to obtain a certain shot limited signal-to-noise ratio.

To obtain a signal-to-noise ratio of 10 for a bandwidth of 40 MHz, the photocathode current must be 10^{-9} amps. For a typical PMT the photocurrent conversion at 0.5145 μ is ~0.06 A/W. Therefore, the power arriving at the photocathode must be $\sim 1.67 \times 10^{-8}$ W. The number of particles required in the probe volume must then be $\sim 1.8 \times 10^6$ particles.

The final step in this preliminary evaluation is to compute the concentration of particles required to obtain the aforementioned number of particles in the probe volume. This computation includes evaluating the extinction due to these particles. For a particle density of 1 g/cm^3 and a particle diameter of 0.65 μ, the particle loading (in kg/m^3) is given by

$$M = 1.4 \times 10^{-10} \times (\text{no. of particles/cm}^3)$$

The extinction length is defined where $I = e^{-1}I_0$ and was obtained using scattering theory. The probe volume was conservatively estimated as

$$PV = (\pi d_w^2/4) \times (\text{extinction length})$$

Table 1 summarizes the computations of extinction length and number of particles in the probe volume as a function of particle concentration.

Requirements of a Pulsed Laser Doppler System

The most important characteristics of the measurement volume are its length, diameter, and fringe spacing. The length is established by the pulse duration, the coherence length, and the imaging optics; the diameter is established by the transmitting optics; and the fringe spacing for a backscattering system is simply one-half of the illumination wavelength. Certain criteria, such as the Nyquist limit, must be met when choosing the optical configuration. There are at least two strategies used to define the laser pulse width.

1) The first strategy is to make the laser pulse width long enough to capture N acoustic cycles, where N is established by signal-to-noise considerations. Furthermore, the diameter of the measurement volume must result in a transit time equivalent to N vibrational cycles. That is, $\tau_{\text{pulse}} \geq N/\nu$ and $d_w \geq NU/\nu$. For instance, to measure $N = 0.5$ for an acoustic frequency of 100 Hz and an air velocity of 1 m/s would require $t_{\text{pulse}} \geq 5$ ms and $d_w \geq 5$ mm. This results in very long pulses that, for all practical purposes, can be considered cw. There are several problems associated with this approach: a) lack of spatial resolution, b) velocity gradients within the probe volume, and c) unresolved turbulence.

2) The second strategy uses modern digital recorders. The Nyquist limit requires digitizing every cycle at least twice. Thus, it should only be necessary to record the bursts coinciding with the required digitizations.[4] In this strategy the laser would be pulsed at rates exceeding twice the measured frequency f_m.

The measured frequency consists of the Doppler frequency added to any frequency shift:

$$f_D = |f_c \pm nf_a|$$

$$f_m = f_D \pm f_s$$

Table 1 Effect of particle concentration on extinction length and number of particles in the probe volume

Particle concentration, cm^{-3}	10^6	10^7	10^8
Particle mass loading, kg/m^3	1.4×10^{-4}	1.4×10^{-3}	1.4×10^{-2}
Extinction length, m	2	0.2	0.02
Number of particles in PV	2×10^6	2×10^6	2×10^6

In backscattering the convective frequency f_c can be in the order of several megahertz, which represents a much higher repetition rate than available lasers. This problem can be avoided by frequency shifting either the reference or the object beam. In the limit the convective term may be eliminated completely leading to a repetition rate RR equal to $RR \geq 2nf_a$.

The laser pulse width should be as narrow as possible. This strategy leads to typical repetition rates in the order of hundreds of hertz and pulse widths between microseconds and nanoseconds. These requirements can be met with available lasers. As mentioned earlier, the probe volume diameter must be large enough to resolve N acoustical cycles over the same sample of particles.

The third important parameter is the fringe spacing. The results of our experiments and numerical model indicate that particles may travel anywhere from a small fraction of a fringe to several fringes. If travel is limited to a fraction of a fringe, most of the energy in the spectrum will be contained by the frequency terms representing the sum and subtraction of the convective frequency and the fundamental acoustic frequency. If the particles cross several fringes, the spectrum will also contain information related to the harmonics of the acoustic frequency. This is manifested as a train of periodic spectra characterized by the expression $|f_c \pm nf_a|$. This periodic information may provide the clearest signature of the presence and position of a helicopter.

Acknowledgments

This work was supported by a Phase I SBIR, Contract DAAH01-90-C-0813, from the U.S. Army Missile Command. The author is extremely grateful to David Rosenthal for enlightening discussions and help in the signal spectral analysis and to Eric Johnson for assistance in the experiments and preparation of this paper.

References

[1]Taylor, K. J., "Absolute Measurement of Acoustic Particle Velocity," *Journal of the Acoustical Society of America,* Vol. 59, No. 3, 1976, pp. 691–694.

[2]Hanish, S., "Underwater Laser Doppler Hydrophone," *Treatise on Acoustic Radiation,* Vol. 2, Naval Research Lab., Washington, DC, 1983, Chap. 6, pp. 377–397.

[3]Vignola, J. F., Berthelot, Y. H., and Jarzynski, J., "Laser Detection of Sound," *Journal of the Acoustical Society of America,* Vol. 90, No. 3, 1991, pp. 1275–1286.

[4]Dopheide, D., Pfeifer, H., Faber, M., and Taux, G., "The Use of High-Frequency Pulsed Laser Diodes in Fringe Type Laser Doppler Anemometry," *Journal of Laser Applications,* Vol. 1, No. 4, 1989, pp. 40–44.